Hindawi
Journal of Food Biochemistry
Volume 2023, Article ID 3788655, 10 pages
https://doi.org/10.1155/2023/3788655

*Research Article*

# Hesperidin Induced HePG-2 Cell Apoptosis through ROS-Mediated p53/Bcl-2/Bax and p-mTOR Signaling Pathways

**Yueyin Pang,[1] Qianlong Wu,[2] Ming Zhang,[3] Jia Lai,[2] Danyang Chen,[2] Jingyao Su,[2] Bing Zhu,[2] Hongmei Zhou,[4] and Yinghua Li[2]**

[1]*Department of Biology, New York University, New York, USA*
[2]*Center Laboratory, Guangzhou Women and Children's Medical Center, Guangzhou Medical University, Guangzhou, China*
[3]*Department of Interventional Radiology and Vascular Anomalies, Guangzhou Medical University, Guangzhou, China*
[4]*Department of Ophthalmology, Guangzhou Women and Children's Medical Center, Guangzhou Medical University, Guangzhou, China*

Correspondence should be addressed to Hongmei Zhou; 472382307@qq.com and Yinghua Li; liyinghua@gzhmu.edu.cn

Received 9 October 2022; Revised 11 November 2022; Accepted 12 November 2022; Published 9 February 2023

Academic Editor: Swapan Ray



Recently, research showed that one of the most common kinds of liver cancer is hepatocellular carcinoma (HCC), which is also the fourth main cause of cancer deaths. In studies regarding chemicals to better treat the disease, hesperidin shows a novel potential in performing anticancer activities, particularly in liver cancer. However, the specific mechanism of hesperidin that causes such activities remains a mystery. Thus, the purpose of this study is to investigate hesperidin's effect on cell proliferation and activation of ROS-mediated signaling pathways in HePG-2 cells. Hesperidin shows a significant impact on inhibiting HePG-2 cells' proliferation through induction of cell apoptosis by Bcl-2, Bax, and p53 pathways. Treating cells with hesperidin in a dose-dependent manner shows a significant increase in the apoptotic cell population (sub-G1). Moreover, Hesperidin's induction of apoptotic activities shows dependence on ROS (reactive oxygen species) overproduction, further affecting the p-mTOR pathways and leading to DNA damage. Hence, the overall data demonstrate that ROS-mediated signaling pathways exhibit mechanisms that may lead to useful information for interpreting hesperidin-induced hepatocarcinoma cell apoptosis.

## 1. Introduction

Cancer is typically defined as the association of diseases with unrestrained cell growth that usually results in metastasis [1]. One of the most common kinds of liver cancer is hepatocellular carcinoma (HCC), which also ranks fourth as the main cause of cancer-related deaths [2, 3]. In the global incidence of hepatocarcinoma, the incidence of hepatocarcinoma is 46.6% and the case fatality rate is 47.1%. Not only that, the age-standardized 5-year survival rate of hepatocarcinoma in the world is only 12.1%. Although the scientific advancement in cancer diagnosis and treatment has significantly improved recently, the problem still exists that many cases of liver cancers with no identified feasible treatment become diagnosed as advanced cancer [4]. Another pessimistic aspect of hepatocarcinoma patients is that this cancer has a high potential for metastasis, as well as a particularly low sensitivity when reacted with chemotherapeutic agents resulting in resistance to conventional cancer drugs [5, 6]. Although the primary purpose of hepatocarcinoma treatment is to kill hepatocarcinoma cells without destroying normal cells, there are still some adverse effects on patients during the treatment of hepatocarcinoma, including anemia, loss of appetite, delirium, and peripheral neuropathy. Moreover, the prevailing causes that impede the performance of the chemotherapeutic method are the low aqueous solubility of many anticancer chemicals and the limited half-life of the agents when positioned the blood circulation [7, 8]. It is thus a demanding cause to discover innovative chemotherapy that can be efficacious for hepatocarcinoma's clinical treatment. Lately, hesperidin has drawn widespread notice for its specific physicochemical

properties, dispersion patterns, stability, size variation, and distribution, morphological characteristics, temperature adaptability, and a crystalline structure that demonstrate the potential of contributing to the chemotherapy field [9]. The expanding application of hesperidin poses optimistic views for using hesperidin as a new option for anticancer drugs [10, 11].

Hesperidin, a flavonoid compound discovered in citrus organisms, is found in common fruits including lemons and oranges. It can also be extracted from *Rutaceae* and *Rubiaceae*, which can reduce capillary brittleness and permeability, diuresis, and analgesia [12]. It has received significant attention because of its anticancerous properties, anti-inflammatory properties, antioxidant roles, and cardioprotective functions in reports [13]. It is also generally applied in food processing because of its bacteriostatic characteristics on certain species [14]. Most importantly, hesperidin displays low cytotoxicity in regular cells, not to mention hesperidin's harmonious effects with many anticancer agents when inhibiting the cell cycle and inducing cell apoptosis in pancreatic cells [15]. Experiments on hesperidin confirm its function to arrest the cell cycle at the G1 phase in prostate and breast cancer cells [16, 17]. Furthermore, recent research shows that hesperidin serves as a possible prevention for the COVID-19 [18]. Hence, the conjecture of hesperidin as a promising chemical agent poses hope and a bright future for advancing chemotherapeutic methods.

Reactive oxygen species (ROS) are oxides that formed from $O_2$'s electron receptivity, including hydrogen peroxide, superoxide, hydroxyl radicals, singlet oxygen, and oxygen free radicals [19]. Oxidative stress, as the notable imbalance, is commonly construed as cellular defense mechanisms or ROS consumption [20]. These oxygen species play a crucial role in numerous physiological processes; thus, the imbalance in a redox reaction can result in various disorders, including the Leigh syndrome, cancerous carcinoma, diabetes, and skin diseases [21]. Though there is research that indicates hesperidin's toxicity to induce oxidative stress, there is little analysis of hesperidin's specific anticancerous mechanisms, especially those of HCC [22]. Investigating the chemotherapeutic aspects of hesperidin will serve a great cause in current hepatocarcinoma clinical treatments. This study aims to examine how hesperidin's effects on the redox reaction balance can regulate HePG-2's mechanism of cell apoptosis and provide a theoretical basis for the development and utilization of therapeutic drugs or adjuvant drugs for hepatocarcinoma.

## 2. Materials and Methods

*2.1. Materials.* HepG-2 cells were provided by American Type Culture Collection (ATCC, Manassas, Virginia). Dulbecco's modified Eagle's medium (DMEM) and fetal bovine serum (FBS) were obtained from Gibco. The p-mTOR, Bcl-2, Bax, P53, caspase-9, and cleaved caspase-3 antibodies were provided by Cell Signaling Technology. Hesperidin was obtained from Sigma. Thiazolyl Blue tetrazolium bromide (MTT), bicinchoninic acid (BCA), 4′6-diamidino-2-phenyindole (DAPI), and propidium iodide (PI) were purchased from Sigma. LysoTracker Deep Red was obtained from Invitrogen. The water used in all experiments was Milli-Q water, purified by Millipore [23].

*2.2. Cell Viability Assay.* HePG-2 cells were incubated in the following conditions: with DMEM supplemented with antibiotics penicillin and streptomycin and 10% FBS in the 37°C humidified incubator with a 5% $CO_2$ atmosphere. The cytotoxicity of hesperidin was determined by performing the cell viability test of the CCK-8 assay as in the previous publication [24]. Briefly, cell viability was calculated by measuring the level of transformation of WST-8 to an orange formazan product inside the cells. HePG-2 cells were cultivated in 96-well culture plates at $5 \times 10^4$ cells per well density in a 37°C incubator for 24 h. This is followed by treating the cells with hesperidin at different concentrations for 24 h. Then, 20 $\mu$l/well of CCK-8 solution and 200 $\mu$l/well of DMEM including 1% FBS were added and placed inside the incubator for another 4 h [19]. After incubation, the medium was replaced with 150 $\mu$l/well DMSO to dissolve the formazan products. Then, the 96-well plate was again placed in the 37°C humidified incubator with a 5% $CO_2$ atmosphere for 2 h. The color intensity of the formazan solution reflects the cell viability, so it was measured at 450 nm using the microplate spectrophotometer (VersaMax). The test was repeated 3 times [25].

*2.3. Flow Cytometric Analysis.* Flow cytometric analysis was implemented to test the effect of hesperidin on cell cycle's distribution as previously stated [26, 27]. In short, after the incubation of hesperidin in HePG-2 cells for 24 h, the cells underwent centrifugation for 5 min at 1500 rpm. The cells were harvested and incubated with precooled 70% ethanol at −20°C for 24 h. The experiment followed 30 min PI staining in the dark. The apoptotic activity of cells and hypodiploid DNA content were assessed by using Multicycle software [28].

*2.4. Annexin-V/PI Double-Staining Assay.* The cells in the logarithmic growth phase were inoculated into a 6-well plate. When collecting the cells, the culture medium was sucked into the centrifuge tube and the cells were washed with PBS. The cells were digested with trypsin without EDTA and collected in the centrifuge tube [29]. Then, the collected medium and cells were mixed well and centrifuged at 4°C for 5 min, and the supernatant was discarded. The cells were washed with precooled PBS 2 times and centrifuged at 4°C for 5 min each time, and the cells were adjusted to the same concentration by adding 1 × binding buffer. $1 \times 10^5$ cell suspensions were taken into the flow tube, and the appropriate amount of Annexin-V labeled with a fluorescent dye and the appropriate amount of PI were added; they were mixed gently and incubated for 15–20 min at room temperature without light. Finally, 300 $\mu$L PBS resuspension cells were added and detected by flow cytometry within 1 hour [30].

*2.5. Cell-Cycle Analysis.* After the cells were stimulated by hesperidin, the culture medium was gently removed, PBS was added to shake gently, and then PBS was removed. 1 mL

trypsin was added, shaken well, and put into the incubator to digest. After digestion, the cells were removed from the incubator and added to a 3 mL medium containing serum to terminate trypsin digestion. The cells were resuspended and transferred to the centrifuge tube using a pipette [31]. Then, the supernatant was removed by 1000 rpm room temperature centrifugation for 5 min, the 3 mL PBS resuspension cells were added, and the supernatant was removed by 1000 rpm normal temperature centrifugation for 5 min. 75% alcohol was added to resuscitate the cells and the cells were placed in a refrigerator at 4°C for the night. 1000 rpm centrifuged 5 min at room temperature, removed the supernatant, added PBS to wash for 3 times, added PI staining solution, stained 30 min at 37°C, and then detected the cell cycle by flow cytometry [32].

*2.6. TUNEL-DAPI Co-Staining Assay.* The TUNEL apoptosis kit detected the effect of hesperidin on DNA fragmentation. PBS was used to wash the cell climbing tablets once, the cells were fixed with 4% paraformaldehyde for 30–60 minutes, and then they were washed again with PBS. Then, PBS containing 0.1% TritionX-100 was added, and it was incubated in the ice bath for 2 minutes and washed with PBS 2 times. Then, 50 $\mu$L TUNEL detection solution was added and incubated at 37°C for 60 minutes. Finally, the film was sealed with an antifluorescence quenching solution and observed under the fluorescence microscope [33].

*2.7. Caspase-3 Activity.* After HepG-2 cells were treated with hesperidin, the cell culture medium was absorbed and set aside. The adherent cells were digested with trypsin and collected into a spare cell culture medium. Then, the cells were collected with 600 g 4°C centrifugation for 5 minutes, the supernatant was carefully removed, while ensuring that no cells are absorbed as far as possible, and it was washed again with PBS [34]. After absorbing the supernatant as before, the lysate was added according to the proportion of 100 microliter lysate for every 2 million cells, resuspended, and cracked in the ice bath for 15 minutes. Then, Ac-DEVD-pNA (2 mM) was added and mixed well and incubated at 37°C for 120 minutes. A405 can be determined by enzyme labeling instruments when the color change is obvious [35].

*2.8. Determination of Reactive Oxygen Species (ROS) Generation.* The hesperidin-induced intracellular ROS generation of treated cells was assessed by DCF fluorescence cell staining as previously reported [36, 37]. In short, harvested cells undergo suspension in PBS with DCFH-DA. 10 mM was the final concentration of DCFH-DA, and the cells were suspended at 37°C for 30 min. After staining, the collected cells were resuspended in PBS. The fluorescence microscope and microplate reader were used to detect the intensity of fluorescence to determine the ROS level. The emission wavelength was excited at 500 nm and 529 nm, respectively. The test was performed 3 times [38].

*2.9. Western Blot Analysis.* Western blot was performed to test the effects of hesperidin on a variety of cellular protein expressions in HePG-2 cells as previously reported [39, 40]. To determine the total cellular proteins, lysis buffer was added to hesperidin-treated HePG-2 cells. BCA assay was performed to determine the protein concentration in cells. 10 $\mu$g of protein was added to each well. Primary antibodies and secondary antibodies at 1 : 1000 dilution inside 5% nonfat milk were added to the membranes. ECL, the enhanced chemiluminescence detection reagent, was used to visualize the protein bands after the incubation.

*2.10. Statistical Analysis.* All tests and experiments were repeated at least 3 times. All data were expressed as mean ± SD. The two-tailed Student's $t$-test was performed to analyze the differences between the experimental group and the control group. Data with differences of $P < 0.05$ ($^*$) or $P < 0.01$ ($^{**}$) were considered statistically significant. For multiple group comparisons, the one-way analysis of the variance method was performed. SPSS 13.0 for Windows was used as the software for performing these analyses.

## 3. Results and Discussion

*3.1. Hesperidin's In Vitro Anticancer Activity.* The cytotoxic activity of hesperidin on HePG-2 cells was determined by a CCK-8 assay. In addition, the concentration gradients of hesperidin determined in this study were derived from preexperiments prior to the formal experiments. In the preexperiment, the investigators used a large number of CCK-8 experiments to find out the optimal concentration range for the effect of hesperidin on HePG-2 cells and LO2 cells. As shown in Figure 1(a), the growth of HePG-2 cells was significantly inhibited by hesperidin in a concentration-dependent manner. HePG-2 cells treated with 160 $\mu$g/mL hesperidin for 24 h have reduced cell viability at 69.53%. The cell viability was reduced to 67.01% and 62.01% as the concentration of hesperidin was increased to 320 $\mu$g/mL and 640 $\mu$g/mL, respectively. In Figure 1(b), hesperidin's anticancer ability becomes further validated. As shown in Figure 1(b), the cytoplasm shrinkage activity emerges in cells treated with hesperidin, as well as loss of intercellular contact. Hence, these results show hesperidin's ability to inhibit cancer cell growth with a dose-dependent treatment.

*3.2. Hesperidin Induction of Cell Apoptosis.* Apoptosis is a critical factor for a wide range of different biological cycles and systems, including the immune system, the embryo development process, the cell cycle, morphological alterations, and chemical-stimulated cell deaths [30]. The decrease of cell membrane potential can be easily detected by the transition of JC-1 from red to green fluorescence. At the same time, JC-1 is an ideal fluorescent probe widely used to detect mitochondrial membrane potential $\Delta\Psi m$. When the mitochondrial membrane potential is high, JC-1 aggregates in the mitochondrial matrix to form a polymer (J-aggregates), which can produce red fluorescence; when the

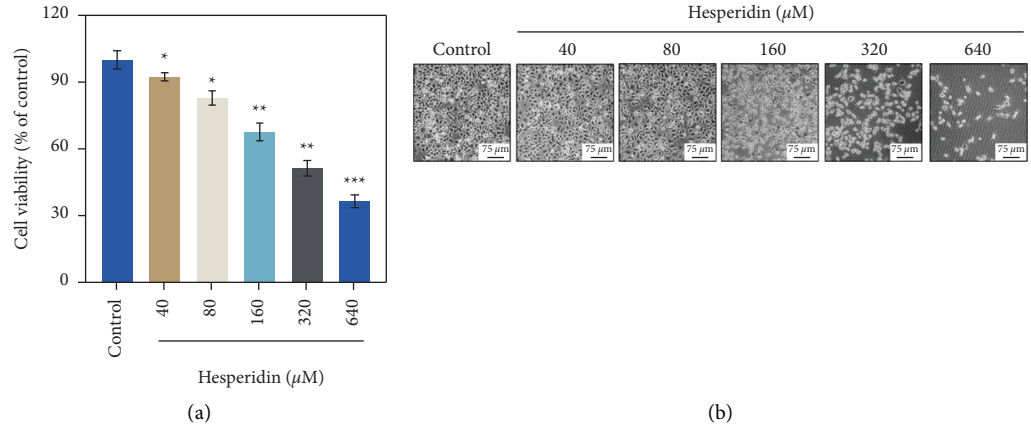


Figure 1: Effects of different concentrations of hesperidin on the growth of HepG-2 and LO2. (a) Cell viability was evaluated after being treated with different concentrations of hesperidin for 24 h by the cell counting kit-8 assay, which was measured at 450 nm using the microplate spectrophotometer (VersaMax). (b) Fluorescence microscope was used to observe morphological changes in HepG-2 cells with different concentrations of hesperidin. The length of the scale plate in the footnote is 75 $\mu$m. Different concentration gradients of hesperidin include 40 $\mu$M, 80 $\mu$M, 160 $\mu$M, 320 $\mu$M, and 640 $\mu$M. Bars with different characters are statistically different at $^{*}P < 0.05$, $^{**}P < 0.01$, and $^{***}P < 0.001$.

mitochondrial membrane potential is low, JC-1 cannot aggregate in the mitochondrial matrix; then JC-1 is a monomer, which can produce green fluorescence. In Figure 2, the results of JC-1 testing of HePG-2 cells incubated with hesperidin for 24 hours are shown. Mitochondrial polarization is indicated by the decreasing ratio of the red/green intensity. Mitochondrial polarization indicates the early stage of cell apoptotic activities.

*3.3. Translocation of Phosphatidylserine Induced by Hesperidin.* Annexin-V/PI double staining flow cytometry is one of the most commonly used methods to detect apoptosis. At the beginning of early apoptosis, phosphatidylserine turns out to the cell surface, that is, the outside of the cell membrane. Annexin-V labeled with green fluorescent probe YF488 can bind to inverted phosphatidylserine to detect the important characteristics of apoptosis. Propidium iodide (PI) is a DNA-binding dye that can stain the nuclei of necrotic cells or cells that lose membrane integrity in the late stage of apoptosis. PI can be excited by a 488, 532, or 546 nm laser, showing red fluorescence. The combination of Annexin-V with phosphatidylserine extroverted to the cell surface can block phosphatidylserine's procoagulant and proinflammatory activity. Annexin-V labeled with green fluorescence probe FITC, namely, Annexin-V-FITC, can be used to detect the extroversion of phosphatidylserine, an essential feature of apoptosis, simply and directly by flow cytometry or using a fluorescence microscope. Therefore, the transfer of phosphatidylserine to the adventitia is critical to the apoptosis of HepG-2 cells. The apoptotic cells induced by hesperidin were detected by Annexin-V/PI double staining. As shown in Figure 3, the dot pattern of the HepG-2 cell treatment group showed that both early apoptotic cells and late apoptotic cells were present. The results showed that hesperidin inhibited the proliferation of HepG-2 cells mainly through apoptosis.

*3.4. Hesperidin-Induced HepG-2 Cell Apoptosis.* Propidium (PI) is a fluorescent dye of double-stranded DNA. The PI method is a classical periodic detection method. Pl is an inserted nucleic acid fluorescent dye, which can selectively bind nucleic acid DNA and RNA double-stranded helix. The amount of binding is proportional to the content of DNA. The distribution of DNA in each stage of the cell cycle can be obtained by flow cytometry, and the percentage content of each stage can be calculated. In apoptotic cells, DNA breaks between nucleosomes to form DNA fragments. Therefore, DNA fragmentation is an important index to judge apoptosis. This study used PI-flow cytometry to analyze whether hesperidin-induced cell death was related to apoptosis. As shown in Figure 4(a), the number of apoptotic cells below G1 in the hesperidin DNA histogram was significantly higher than that in the control group. For example, in HepG-2 cells treated with different concentrations of hesperidin, the number of apoptotic cells increased sharply from 35.7% to 51.7%. There was no significant change in G0/G1, S, and G2/M phases.

When apoptosis occurs, cells activate some DNA endonucleases, which can cause double- or single-strand breaks of chromosome DNA to produce a large number of sticky 3′-OH ends. Under the action of deoxyribonucleotide terminal transferase (TdT), deoxyribonucleotides and derivatives formed by fluorescein, peroxidase, alkaline phosphatase, or biotin can be labeled to the 3′ end of DNA. Therefore, TUNEL staining is a terminal transferase marker, accurately reflecting apoptotic cells'

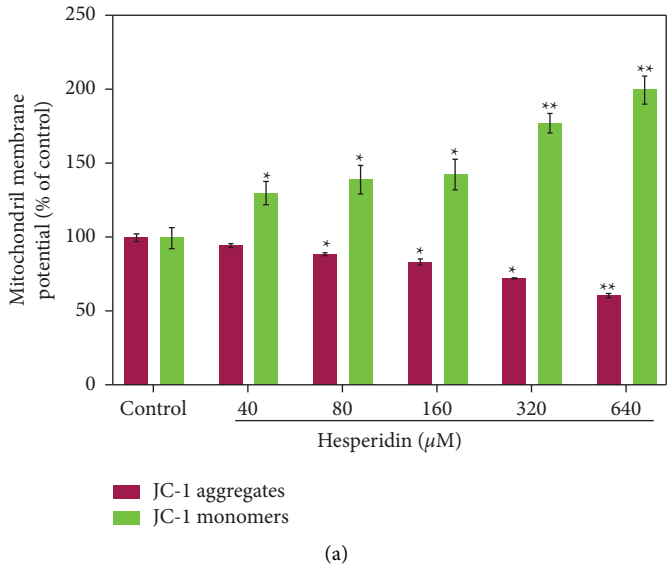


(a)

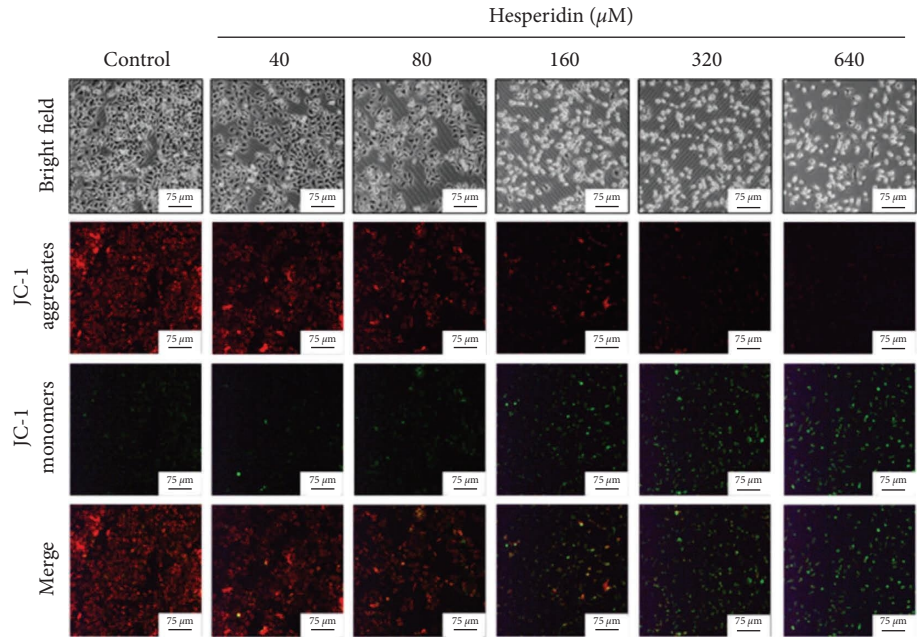


(b)

Figure 2: Depletion of mitochondrial membrane potential induced by different concentrations of hesperidin. (a) The percentage of mitochondrial membrane potential, which was measured at 485 nm and 530 nm using the microplate spectrophotometer (VersaMax). The red bar represents JC-1 aggregates, and the green bar represents JC-1 monomers. (b) JC-1 aggregates and monomers of HepG-2 were exposed to different concentrations of hesperidin under the fluorescence microscope. It was observed that with the increase of hesperidin concentration, JC-1 aggregates (red fluorescence) decreased, while JC-1 monomers (green fluorescence) increased, indicating that mitochondrial permeability increased and mitochondrial membrane potential decreased gradually. The length of the scale plate in the footnote is 75 $\mu$m. Different concentration gradients of hesperidin include 40 $\mu$M, 80 $\mu$M, 160 $\mu$M, 320 $\mu$M, and 640 $\mu$M. Bars with different characters are statistically different at $^{*}P < 0.05$ and $^{**}P < 0.01$.

biochemical and morphological characteristics. As shown in Figure 4(b), HepG-2 cells showed the features of apoptosis, DNA fragmentation, and nuclear condensation under the action of hesperidin. It can be seen from Figure 4(b) that hesperidin induces apoptosis in HepG-2 cells.

*3.5. Detection of Caspase-3 Activity.* The caspase family plays a very important role in mediating apoptosis, in which caspase-3 is a key executive molecule, which plays a role in many pathways of apoptosis signal transduction. Caspase-3 normally exists in the cytoplasm in the form of zymogen (32

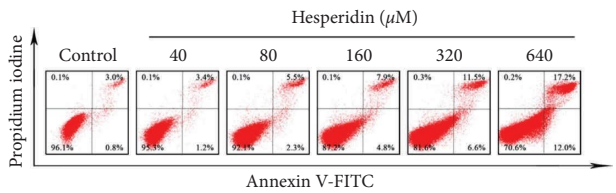


Figure 3: Translocation of phosphatidylserine induced by different concentrations of hesperidin in HepG-2 cells. Normal cells are depicted in the lower left quadrant, late apoptotic cells are depicted in the upper right quadrant, and early apoptotic cells are depicted in the lower right quadrant. The upper right quadrant indicated cells in the early stage of apoptosis, and the lower right quadrant shows cells in the late stage of apoptosis or necrosis. Different concentration gradients of hesperidin include 40 $\mu$M, 80 $\mu$M, 160 $\mu$M, 320 $\mu$M, and 640 $\mu$M. It was observed that the number of apoptotic cells increased with the increase of hesperidin concentration.

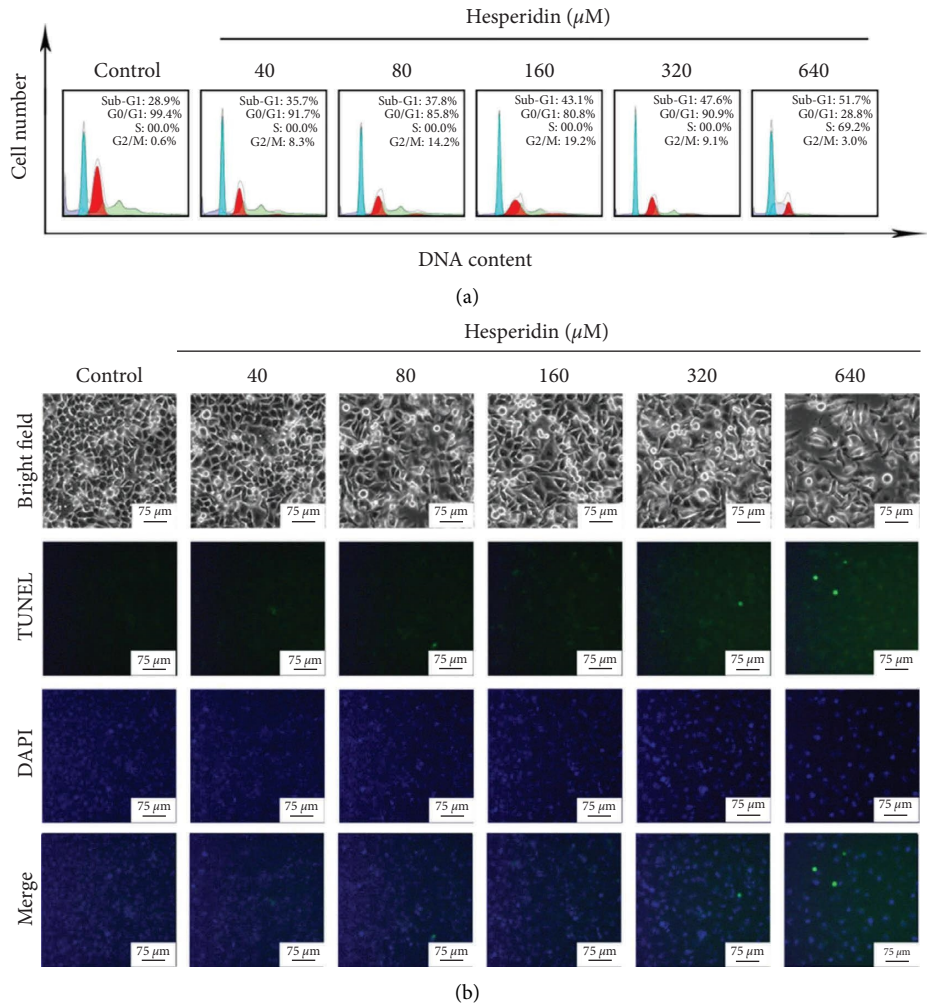


Figure 4: Hesperidin-induced apoptosis in HepG-2 cells. (a) The cell-cycle distribution with different concentrations of hesperidin was analyzed by quantifying DNA content using flow cytometric analysis. The sub-G1 peak on the fluorogram detected by flow cytometry is the apoptotic cell peak. The number marked in the upper right corner of each box is the result of its quantitative analysis for each cell cycle. (b) Representative photomicrographs of DNA fragmentation and nuclear condensation as detected by the TUNEL-DAPI co-staining assay under the fluorescence microscope. The length of the scale plate in the footnote is 75 $\mu$m. Different concentration gradients of hesperidin include 40 $\mu$M, 80 $\mu$M, 160 $\mu$M, 320 $\mu$M, and 640 $\mu$M.

KD). In the early stage of apoptosis, it is activated. The activated caspase-3 consists of two large subunits (17 KD) and two small subunits (12 KD), with cleavage of the corresponding cytoplasmic nuclear substrate, and eventually leads to apoptosis. Caspase-3 can cleave procaspase 2, 6, 7, and 9 and can directly and specifically cleave many caspase substrates, including PARP (poly (ADP-ribose) polymerase), ICAD (Inhibitor of caspase-activated deoxyribonuclease), gelsolin, and fodrin. This caspase-3-mediated protein splicing is an important part of the

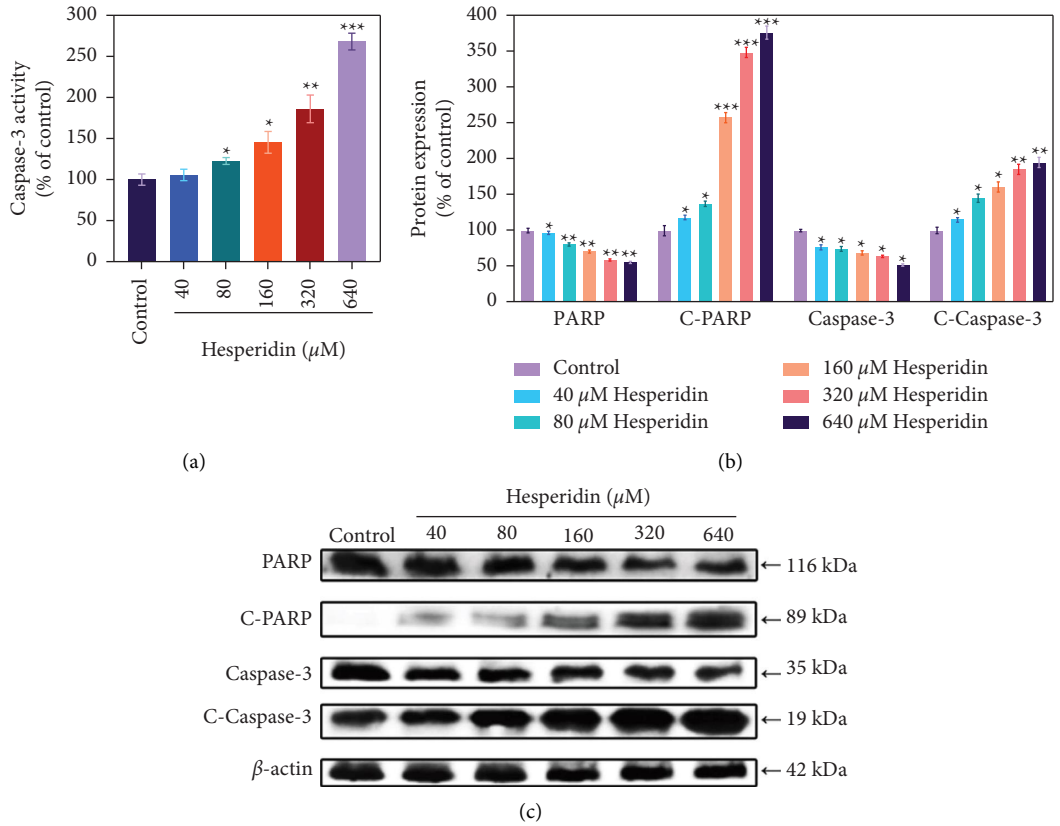


Figure 5: Caspase-3 and PARP-mediated apoptosis induced by Hesperidin in HepG-2 cells. (a) The synthetic fluorogenic substrate analyzed HepG-2 cells treated with hesperidin and caspase-3 activity, which was measured at 405 nm using the microplate spectrophotometer (VersaMax). (b) The expression of PARP, C-PARP, Caspase-3, and C-Caspase-3 by western blot; $\beta$-actin was used as the loading control. (c) Bands were quantified by Image J and results are expressed as a percentage of control. Different concentration gradients of hesperidin include 40 $\mu$M, 80 $\mu$M, 160 $\mu$M, 320 $\mu$M, and 640 $\mu$M. Bars with different characters are statistically different at $^{*}P < 0.05$, $^{**}P < 0.01$, and $^{***}P < 0.001$.

molecular mechanism of apoptosis. However, in the late stage of apoptosis and dead cells, the activity of caspase-3 decreased significantly. PARP is one of the main cleavage targets of caspase-3 and is located downstream of caspase family proteins in the apoptosis pathway. Apoptosis was detected by inhibiting the activation of caspase-3. In this study, HepG-2 cells were treated with different concentrations of hesperidin. An enzyme labeling instrument detected the activity of caspase-3. As shown in Figure 5(a), the caspase-3 activity of the control group of uninfected cells was 100%. Compared with the control group, the hesperidin treatment group increased significantly, being 105.7% (40 $\mu$M), 122.9% (80 $\mu$M), 145.2% (160 $\mu$M), 186.2% (320 $\mu$M), and 268.1% (640 $\mu$M), respectively. Caspase-3 and subsequent PARP cleavage were detected by western blotting to evaluate its participation and contribution to apoptosis. As shown in Figures 5(b) and 5(c), the expression levels of caspase-3 and PARP were downregulated after hesperidin treatment. Not only that, but hesperidin also upregulated the expression level of caspase-3 and PARP. The results showed that hesperidin significantly enhanced the activation of caspase-3 and the cleavage of downstream PARP. These results suggest that hesperidin may induce apoptosis through caspase-3.

*3.6. Hesperidin Induction of ROS Generation.* ROS is a ubiquitous metabolite in organisms, which mainly comes from the respiratory system of mitochondria. In the middle of the respiratory chain of mitochondria, oxygen is reduced to ROS. In addition, NADPH oxidase on the plasma membrane and cytochrome P450 oxidoreductase in the cytoplasm can also convert oxygen into reactive oxygen species. Moderate ROS plays an important role in maintaining the normal physiological function of the body. When the body is affected by disease and oxidative stress, the production of ROS will increase, and these excess ROS will attack biological macromolecules, such as DNA, lipids, and proteins, resulting in damage to their structure and function. As a kind of intracellular signal molecule, ROS participates in the key link of cell signal transduction. A large number of studies have shown that too much ROS will cause oxidative damage to macromolecules in cells, thus inhibiting the role of proteins and then accelerating cell apoptosis and autophagy [41]. Hence, in this experiment, a DCF fluorescence assay was performed to measure the ROS generation to reveal hesperidin's role and action mechanisms in cell apoptosis. As shown in Figure 6, intracellular ROS generation is increased by the addition of hesperidin in HePG-2 cells. The level of intracellular ROS generation is raised to 103% at

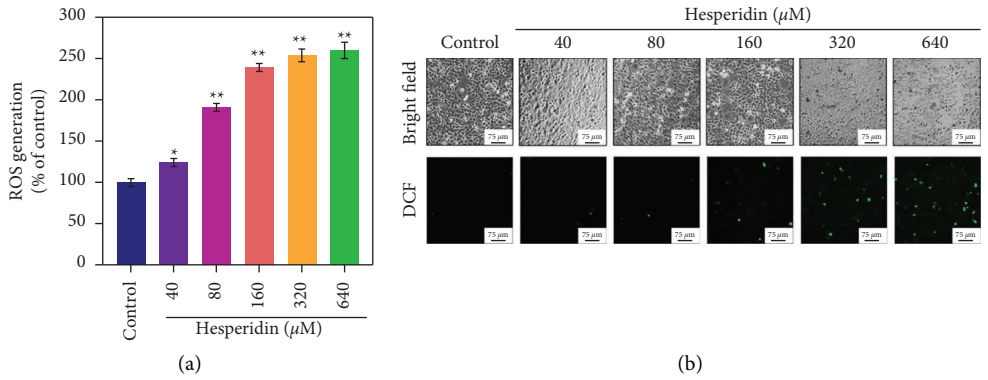


Figure 6: ROS overproduction induced by hesperidin of HepG-2 cells. (a) Changes in intracellular ROS generation detected by measuring DCF fluorescence intensity, which was measured at 500 nm using the microplate spectrophotometer (VersaMax). (b) HepG-2 cells were incubated with ten $\mu$M DCF-DA in PBS for 30 min and then treated with different concentrations of hesperidin under a phase-contrast microscope. The length of the scale plate in the footnote is 75 $\mu$m. Different concentration gradients of hesperidin include 40 $\mu$M, 80 $\mu$M, 160 $\mu$M, 320 $\mu$M, and 640 $\mu$M. Bars with different characters are statistically different at $^{*}P < 0.05$ and $^{**}P < 0.01$.

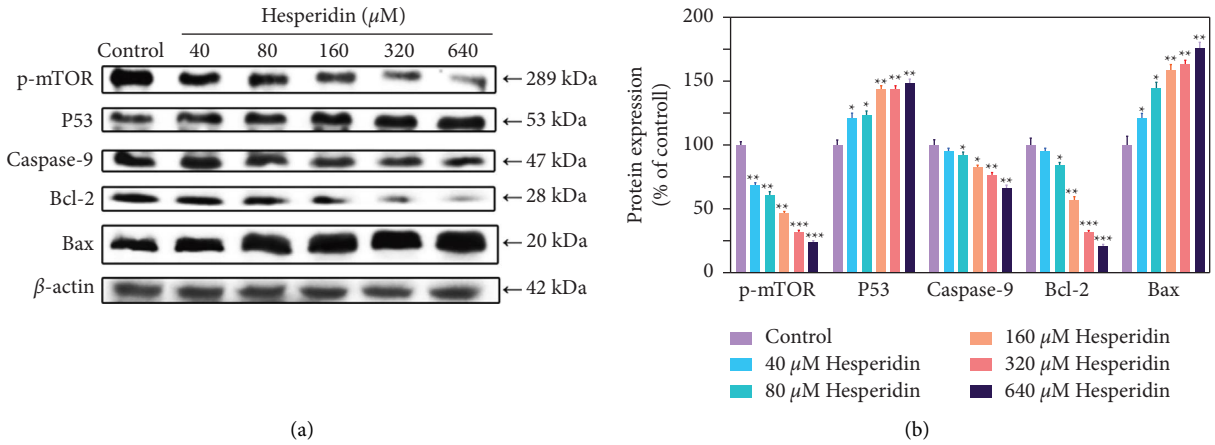


Figure 7: Activation of intracellular apoptotic signaling pathways by hesperidin in HepG-2 cells. (a) The expression level of p-mTOR, P53, Caspase-9, Bcl-2, and Bax in hesperidin treated HePG-2 cells. Through densitometry analysis, the number above the bands is determined to present the protein expression levels. (b) Bands were quantified by Image J and results are expressed as a percentage of control; $\beta$-actin was used as the loading control. Bars with different characters are statistically different at $^{*}P < 0.05$, $^{**}P < 0.01$, and $^{***}P < 0.001$.

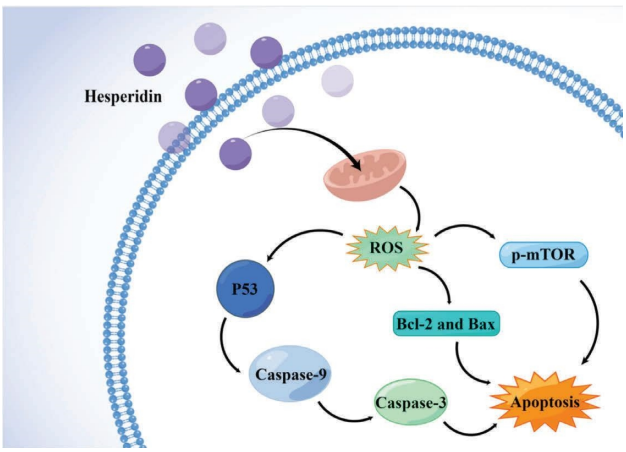


Figure 8: Apoptotic signaling pathways regulated by hesperidin in HepG-2 cells. The main signaling pathway of ROS-mediated p53, p-mTOR, Bcl-2, and Bax signaling pathways. Directional arrows represent agitation.

a hesperidin concentration of 320 $\mu$g/mL. These data confirm that the involvement of ROS generation would have an important impact on the anticancer activity of Hesperidin.

*3.7. Activation of ROS-Mediated Signaling Pathways by Hesperidin.* The activation of p-mTOR, p53, Bcl-2, and Bax signaling pathways caused by intracellular ROS overflow can trigger apoptotic activities. Western blot was performed to characterize the effects triggered by hesperidin on the ROS-mediated downstream passage. As shown in Figure 7, hesperidin-treated HePG-2 cells increased p53 expression levels significantly. Furthermore, there are differential activities triggered by hesperidin on p-mTOR and caspase-9. While hesperidin significantly increased the Bax, HePG-2 cells receiving treatment with hesperidin have displayed decreased expression levels of the protein Bcl-2. As a result, these data establish that hesperidin regulates ROS-mediated p-mTOR, p53, Bcl-2, and Bax signaling pathways to induce apoptotic activities in HePG-2 cells. In summary, hesperidin induces apoptosis in HepG-2 cells by regulating ROS-mediated p53, p-mTOR, Bcl-2, and Bax signaling pathways (Figure 8).

## 4. Conclusions

To summarize the study, it describes a preparation of hesperidin that triggers a simple chemical method under a redox system. Hesperidin exhibits a great potential to inhibit HePG-2 cell proliferation with anticancer activity. The main conclusions are as follows: Hesperidin can inhibit the proliferation of HePG-2 hepatoma cells by inducing apoptosis. After hesperidin treatment, the cells became round, the cell membrane permeability increased, the nucleus showed pyknosis, the DNA showed fragmentation, and the cells showed typical characteristics of apoptosis. Hesperidin induces intracellular ROS production by reducing the mitochondrial membrane potential. The molecular mechanisms confirm hesperidin's activation of STAT-3-mediated apoptosis by triggering intracellular ROS overproduction. Further examinations show hesperidin triggers p-AKT and p38 apoptotic signaling pathways in HePG-2 cells. Hence, the study finds that hesperidin exhibits potential anticancer properties.

## Data Availability

No underlying data were collected or produced in this study.

## Conflicts of Interest

The authors declare that they have no conflicts of interest in this work.

## Authors' Contributions

Yueyin Pang, Qianlong Wu, and Ming Zhang contributed equally to the work. Yueyin Pang, Qianlong Wu, and Ming Zhang designed the study, analyzed the experimental data, and drafted the manuscript. Danyang and Jingyao Su carried out the experiments. Bing Zhu and Hongmei Zhou analyzed the data and drafted the manuscript. Yinghua Li refined the manuscript and coordination. All authors read and approved the final manuscript.

## Acknowledgments

This work was supported by the Science and Technology Planning Project of Guangzhou (202201020655 and 202102010202), the Guangdong Natural Science Foundation (2020A1515110648), the Open Fund of Guangdong Provincial Key Laboratory of Functional Supramolecular Coordination Materials and Applications (2020A03), the Guangzhou Medical University Students' Science and Technology Innovation Project (02-408-2203-2079 and 2021AEK119), and Open Project of Guangdong Key Laboratory of Marine Materia Medica (LMM2020-7).

## References

[1] D. Hanahan and R. A. Weinberg, "The hallmarks of cancer," *Cell*, vol. 100, no. 1, pp. 57–70, 2000.

[2] Z. Liu, C. Suo, X. Mao et al., "Global incidence trends in primary liver cancer by age at diagnosis, sex, region, and etiology, 1990-2017," *Cancer*, vol. 126, no. 10, pp. 2267–2278, 2020.

[3] C. Mattiuzzi and G. Lippi, "Current cancer epidemiology," *Journal of Epidemiology and Global Health*, vol. 9, no. 4, pp. 217–222, 2019.

[4] M. Cervello, M. R. Emma, G. Augello et al., "New landscapes and horizons in hepatocellular carcinoma therapy," *Aging (Albany NY)*, vol. 12, no. 3, pp. 3053–3094, 2020.

[5] D. Ling, H. Xia, W. Park et al., "pH-sensitive nanoformulated triptolide as a targeted therapeutic strategy for hepatocellular carcinoma," *ACS Nano*, vol. 8, no. 8, pp. 8027–8039, 2014.

[6] R. K. Thapa, J. Y. Choi, B. K. Poudel et al., "Multilayer-coated liquid crystalline nanoparticles for effective sorafenib delivery to hepatocellular carcinoma," *ACS Applied Materials & Interfaces*, vol. 7, no. 36, pp. 20360–20368, 2015.

[7] L. Li, H. Wang, Z. Y. Ong et al., "Polymer- and lipid-based nanoparticle therapeutics for the treatment of liver diseases," *Nano Today*, vol. 5, no. 4, pp. 296–312, 2010.

[8] H. Wang, C. A. Thorling, X. Liang et al., "Diagnostic imaging and therapeutic application of nanoparticles targeting the liver," *Journal of Materials Chemistry B*, vol. 3, no. 6, pp. 939–958, 2015.

[9] A. Ghorbani, M. Nazari, M. Jeddi-Tehrani, and H. Zand, "The citrus flavonoid hesperidin induces p53 and inhibits NF-$\kappa$B activation in order to trigger apoptosis in NALM-6 cells: involvement of PPAR$\gamma$-dependent mechanism," *European Journal of Nutrition*, vol. 51, no. 1, pp. 39–46, 2012.

[10] S. Baek, R. K. Singh, D. Khanal et al., "Smart multifunctional drug delivery towards anticancer therapy harmonized in mesoporous nanoparticles," *Nanoscale*, vol. 7, no. 34, pp. 14191–14216, 2015.

[11] V. Biju, "Chemical modifications and bioconjugate reactions of nanomaterials for sensing, imaging, drug delivery and therapy," *Chemical Society Reviews*, vol. 43, no. 3, pp. 744–764, 2014.

[12] H. Parhiz, A. Roohbakhsh, F. Soltani, R. Rezaee, and M. Iranshahi, "Antioxidant and anti-inflammatory properties of the citrus flavonoids hesperidin and hesperetin: an updated review of their molecular mechanisms and experimental

models," *Phytotherapy Research*, vol. 29, no. 3, pp. 323–331, 2015.

[13] C. Li and H. Schluesener, "Health-promoting effects of the citrus flavanone hesperidin," *Critical Reviews in Food Science and Nutrition*, vol. 57, no. 3, pp. 613–631, 2017.

[14] F. R. Stermitz, K. K. Cashman, K. M. Halligan, C. Morel, G. P. Tegos, and K. Lewis, "Polyacylated neohesperidosides from Geranium caespitosum: bacterial multidrug resistance pump inhibitors," *Bioorganic & Medicinal Chemistry Letters*, vol. 13, no. 11, pp. 1915–1918, 2003.

[15] J. Lee, J. Lee, M. Kim, and J. H. Kim, "Dietary approach to attenuate human pancreatic cancer growth and migration with innoxiousness," *Journal of Functional Foods*, vol. 30, pp. 303–312, 2017.

[16] E. J. Choi, "Hesperetin induced G1-phase cell cycle arrest in human breast cancer MCF-7 cells: involvement of CDK4 and p21," *Nutrition and Cancer*, vol. 59, no. 1, pp. 115–119, 2007.

[17] C. J. Lee, L. Wilson, M. A. Jordan, V. Nguyen, J. Tang, and G. Smiyun, "Hesperidin suppressed proliferations of both human breast cancer and androgen-dependent prostate cancer cells," *Phytotherapy Research*, vol. 24, no. S1, pp. S15–S19, 2010.

[18] P. Bellavite and A. Donzelli, "Hesperidin and SARS-CoV-2: new light on the healthy function of citrus fruits," *Antioxidants*, vol. 9, no. 8, p. 742, 2020.

[19] Y. Li, X. Li, W. Zheng, C. Fan, Y. Zhang, and T. Chen, "Functionalized selenium nanoparticles with nephroprotective activity, the important roles of ROS-mediated signaling pathways," *Journal of Materials Chemistry B*, vol. 1, no. 46, pp. 6365–6372, 2013.

[20] Y. Li, X. Li, Y. S. Wong et al., "The reversal of cisplatin-induced nephrotoxicity by selenium nanoparticles functionalized with 11-mercapto-1-undecanol by inhibition of ROS-mediated apoptosis," *Biomaterials*, vol. 32, no. 34, pp. 9068–9076, 2011.

[21] M. Zuberek, D. Wojciechowska, D. Krzyzanowski, S. Meczynska-Wielgosz, M. Kruszewski, and A. Grzelak, "Glucose availability determines silver nanoparticles toxicity in HepG2," *Journal of Nanobiotechnology*, vol. 13, no. 1, p. 72, 2015.

[22] P. V. AshaRani, G. Low Kah Mun, M. P. Hande, and S. Valiyaveettil, "Cytotoxicity and genotoxicity of silver nanoparticles in human cells," *ACS Nano*, vol. 3, no. 2, pp. 279–290, 2009.

[23] M. Pi, K. Kapoor, R. Ye, J. C. Smith, J. Baudry, and L. D. Quarles, "GPCR6A is a molecular target for the natural products gallate and EGCG in green tea," *Molecular Nutrition & Food Research*, vol. 62, no. 8, Article ID e1700770, 2018.

[24] F. Yang, Q. Tang, X. Zhong, Y. Bai, T. Chen, and Y. Zhang, "Surface decoration by Spirulina polysaccharide enhances the cellular uptake and anticancer efficacy of selenium nanoparticles," *International Journal of Nanomedicine*, vol. 7, pp. 835–844, 2012.

[25] Y. Xie, C. Mu, B. Kazybay et al., "Network pharmacology and experimental investigation of Rhizoma polygonati extract targeted kinase with herbzyme activity for potent drug delivery," *Drug Delivery*, vol. 28, no. 1, pp. 2187–2197, 2021.

[26] W. Jiang, Y. Fu, F. Yang et al., "Gracilaria lemaneiformis polysaccharide as integrin-targeting surface decorator of selenium nanoparticles to achieve enhanced anticancer efficacy," *ACS Applied Materials & Interfaces*, vol. 6, no. 16, pp. 13738–13748, 2014.

[27] Y. Xia, P. You, F. Xu, J. Liu, and F. Xing, "Novel functionalized selenium nanoparticles for enhanced anti-hepatocarcinoma activity in vitro," *Nanoscale Research Letters*, vol. 10, no. 1, p. 349, 2015.

[28] Y. Li, T. Xu, Z. Lin et al., "Inhibition of enterovirus A71 by selenium nanoparticles interferes with JNK signaling pathways," *ACS Omega*, vol. 4, no. 4, pp. 6720–6725, 2019.

[29] T. Nie, H. Wu, K. H. Wong, and T. Chen, "Facile synthesis of highly uniform selenium nanoparticles using glucose as the reductant and surface decorator to induce cancer cell apoptosis," *Journal of Materials Chemistry B*, vol. 4, no. 13, pp. 2351–2358, 2016.

[30] Y. Li, M. Guo, Z. Lin et al., "Multifunctional selenium nanoparticles with Galangin-induced HepG2 cell apoptosis through p38 and AKT signalling pathway," *Royal Society Open Science*, vol. 5, no. 11, Article ID 180509, 2018.

[31] L. Xie, Z. Luo, Z. Zhao, and T. Chen, "Anticancer and antiangiogenic iron(II) complexes that target thioredoxin reductase to trigger cancer cell apoptosis," *Journal of Medicinal Chemistry*, vol. 60, no. 1, pp. 202–214, 2017.

[32] V. A. D'Yakonov, A. A. Makarov, L. U. Dzhemileva, I. R. Ramazanov, E. K. Makarova, and U. M. Dzhemilev, "Natural trienoic acids as anticancer agents: first stereoselective synthesis, cell cycle analysis, induction of apoptosis, cell signaling and mitochondrial targeting studies," *Cancers*, vol. 13, no. 8, p. 1808, 2021.

[33] C. L. Moore, A. V. Savenka, and A. G. Basnakian, "TUNEL assay: a powerful tool for kidney injury evaluation," *International Journal of Molecular Sciences*, vol. 22, no. 1, p. 412, 2021.

[34] Y. Xu, H. Li, J. Liang et al., "High-throughput quantification of eighteen heterocyclic aromatic amines in roasted and pan-fried meat on the basis of high performance liquid chromatography-quadrupole-orbitrap high resolution mass spectrometry," *Food Chemistry*, vol. 361, Article ID 130147, 2021.

[35] H. Chen, J. Zhang, Y. Gao et al., "Sensitive cell apoptosis assay based on caspase-3 activity detection with graphene oxide-assisted electrochemical signal amplification," *Biosensors and Bioelectronics*, vol. 68, pp. 777–782, 2015.

[36] T. Liu, L. Zeng, W. Jiang, Y. Fu, W. Zheng, and T. Chen, "Rational design of cancer-targeted selenium nanoparticles to antagonize multidrug resistance in cancer cells," *Nanomedicine: Nanotechnology, Biology and Medicine*, vol. 11, no. 4, pp. 947–958, 2015.

[37] G. Newham, R. K. Mathew, H. Wurdak, S. D. Evans, and Z. Y. Ong, "Polyelectrolyte complex templated synthesis of monodisperse, sub-100 nm porous silica nanoparticles for cancer targeted and stimuli-responsive drug delivery," *Journal of Colloid and Interface Science*, vol. 584, pp. 669–683, 2021.

[38] Y. Feng, J. Su, Z. Zhao et al., "Differential effects of amino acid surface decoration on the anticancer efficacy of selenium nanoparticles," *Dalton Transactions*, vol. 43, no. 4, pp. 1854–1861, 2014.

[39] Y. Huang, L. He, W. Liu et al., "Selective cellular uptake and induction of apoptosis of cancer-targeted selenium nanoparticles," *Biomaterials*, vol. 34, no. 29, pp. 7106–7116, 2013.

[40] Y. B. Wang, J. Qin, X. Y. Zheng, Y. Bai, K. Yang, and L. P. Xie, "Diallyl trisulfide induces Bcl-2 and caspase-3-dependent apoptosis via downregulation of Akt phosphorylation in human T24 bladder cancer cells," *Phytomedicine*, vol. 17, no. 5, pp. 363–368, 2010.

[41] W. Liu, X. Li, Y. S. Wong et al., "Selenium nanoparticles as a carrier of 5-fluorouracil to achieve anticancer synergism," *ACS Nano*, vol. 6, no. 8, pp. 6578–6591, 2012.